



# Micro-machining of UHMWPE composites reinforced with carbide fillers

Selim Gürge<sup>1</sup> · Mehmet Alper Sofuoğlu<sup>2</sup>

Received: 8 April 2021 / Revised: 18 June 2021 / Accepted: 2 September 2021 / Published online: 10 September 2021  
© Wrocław University of Science and Technology 2021

## Abstract

Polymer matrix composites (PMCs) have become one of the most widely used engineering materials due to both the developments in polymers and advanced fillers. It is expected that polymer composites will take their final shape during the production phase, which means that they are not required to undergo new processes. However, in some applications, machining operations, such as turning, milling, grooving and hole drilling, cannot be avoided and thus, finishing operations must be applied to these materials. Since these materials have complex microstructures, finishing operations may cause situations that adversely affect engineering properties, such as matrix cracking, delamination, debonding, etc. In this study, micro-milling operations were performed for recently developed ceramic reinforced polymer composites. Three different spindle speeds were used while feed rate and cutting depth were kept constant in the operations. The composites were produced from powdered UHMWPE and silicon carbide particles. Several parameters were varied in the production of the composites, such as molding pressure, filler loading and filler size. The investigated outputs were cutting temperature and surface roughness, whereas machined surfaces and chip morphologies were also investigated via microscopy analyses. In the final stage, regression analyses were performed to investigate the relationships between the process parameters. According to the results, ceramic reinforced polymer composites exhibit different machinability properties than fiber-reinforced ones due to hard fillers and low melting point of UHMWPE.

**Keywords** Micro-machining · Polymer composites · UHMWPE · Carbide fillers

## Abbreviations

ANOVA	Analysis of variance
CFRP	Carbon fiber-reinforced polymer
EDS	Energy-dispersive spectrometry
PMC	Polymer matrix composite
SEM	Scanning electron microscopy
SiC	Silicon carbide
UHMWPE	Ultra-high molecular weight polyethylene

## 1 Introduction

Micro-machining plays a significant role in the miniaturization of products. Micro-manufacturing aims to produce small-sized parts that shrink the entire production process, taking up less space and consuming fewer resources and energy [1]. This results in lower energy consumption, fewer material requirements, less noise and pollution, and ultimately facilitating a more environmentally friendly machining process [2]. The topic of micro-manufacturing has been discussed by numerous authors, as reported in previous studies [3]. It is stated that the effect of miniaturization and a 1/10 reduction of the production plant could lead to a 1/100 decrease in energy consumption [4]. The most striking improvement in micro-manufacturing is the ability to produce components with a characteristic size of 100 µm close to human hair size [5].

In recent years, the use of polymer matrix composites has increased in several fields of science and technology due to their advanced physical and mechanical properties. These composites are characterized by the hybridization of

✉ Selim Gürge  
sgurgen@ogu.edu.tr

<sup>1</sup> Department of Aeronautical Engineering, Eskişehir Osmangazi University, Eskişehir, Turkey

<sup>2</sup> Department of Mechanical Engineering, Eskişehir Osmangazi University, Eskişehir, Turkey

lightweight, very high strength and stiffness, so they have replaced traditional metallic materials [6]. Because of these features and potential applications in aerospace, automotive and biomedical industries, there is a need to be understood in areas such as machining. Machining of composites is essential to finish the products to the desired tolerances and prepare them for subsequent assemblies. Traditional machining operations are used to produce complex features by removing material. Unlike metals, polymer-based composites are generally non-homogeneous materials, which show anisotropic properties. For this reason, metal machining is different than the machining of polymer composites in great measure. Surface quality and cutting forces are profoundly affected by filler ratio, shape and orientation [7]. In the requirements of polymer composites for machining, low material removal rates and lower cutting temperatures are desired. In general, composite machining is considered a finishing operation and, uncut chip thickness, chip removal rates and cutting forces are lower than metal machining operations [8].

Hocheng [9] carried out milling operation of carbon fiber-reinforced polymer (CFRP) composites and investigated tool-wear performance of uncoated and diamond-coated carbide end mills. Sheikh-Ahmad et al. [10] proposed a mechanistic modeling method to calculate cutting forces and simulate the milling operation of unidirectional/multidirectional polymer composites. Multiple regression and neural network techniques were benefitted using milling force data. A new cutting model was proposed to calculate the cutting forces at different fiber orientations. Gara et al. [11] investigated the slotting of polymer composites via knurled tools and suggested a model in terms of surface roughness. It was stated that the feed per tooth has a significant effect on surface quality. A knurled tool with fine teeth is appropriate for the slotting since less damage was observed. An empirical study for the machining of laminated composites was conducted in an early work [12] to find the surface quality and cutting temperatures. Different empirical models were developed to investigate the effects of cutting parameters on cutting temperature. Azmi et al. [13] investigated an end milling operation to determine the machinability of polymer composites. A hybrid method was studied and multiple regression analysis was used to determine the effects of process inputs on the machinability. They concluded that feed rate and spindle speed have significant impacts on surface quality. Ghafarizadeh et al. [14] developed a numerical model to study the flat end milling of CFRP composites. The model was validated in terms of cutting forces and machined surfaces. It was stated that fiber orientation affects the extension of machining damage. He et al. [15] carried out the slot milling of laminated composites to propose a mechanistic milling force model. They found that the

effect of instantaneous fiber orientation angle and chip thickness on tangential/radial forces are significant. Pecat et al. [16] conducted research on milling of CFRP composites at high machining speeds to investigate the cutting process for specific fiber orientation angles. Iskandar et al. [17] investigated the lubrication role in the milling of polymeric laminates. From this study, wear on the cutting tool is suppressed by a ratio of 22% in lubricating conditions. Hintze et al. [18] studied the material integrity of laminated composites in milling operations. Delamination and fiber protrusions are the typical damages that can be observed at several ranges of the fiber orientation angle. Szallies et al. [19] conducted a low-frequency oscillated milling for CFRP composites using a special carbide tool. It was stated that delamination is lower in oscillatory milling comparing to conventional milling.

Although there are several studies on the machining operation of polymer composites, the majority of these works focus on fiber-reinforced polymer composites. However, in recent studies, polymer matrix composites reinforced with ceramic fillers have been attracted much attention due to their advanced mechanical, thermal, electrical and tribological properties [20]. For example, these composites are designed for covering or casing materials in micro-electronics applications. Although the primary function of covering is to protect electronic devices from various environmental conditions, such as moisture, dust, chemical agents and light, miniaturization of micro-electronics demands multifunctional materials such as being capable of heat dissipation while insulating electricity in addition to conventional protection properties. For this reason, ceramic reinforced polymer composites are highly demanded by the microelectronics industry [21]. Machining of this group of composites is a novel subject and therefore, we investigated the micro-milling behavior of silicon carbide (SiC) filled ultra-high molecular weight polyethylene (UHMWPE) composites in this study. The machined composites were produced from powdered UHMWPE and particulate carbide fillers in a compression molding chamber. Compression pressure was varied in the molding process to investigate the influence of molding pressure on machinability performance. The composition of specimens was also changed using different filler amount and filler size to observe their roles in the milling operation. Each of the specimens was machined at three different spindle speeds while feed rate and depth of cut were kept constant. Cutting temperature and surface roughness were measured and evaluated as the process outputs. In the final stage, a non-linear regression analysis was performed to investigate the relation between these parameters. From the results, ceramic reinforced polymer composites exhibit different machinability properties than fiber-reinforced ones because soft polymer matrix has ductile properties; however, hard ceramic fillers develop frictional interactions in

the soft matrix. Moreover, UHMWPE shows melting rather than thermal softening in some machining cases since the melting point of this polymer is quite low.

## 2 Experimental details

### 2.1 Materials and specimen preparation

In this study, powdered UHMWPE (43,951, Alfa Aesar) with a molecular weight of 3–6 million g/mol was used as the polymer matrix in the specimens. Three different particle sizes (0.3, 0.5 and 1.0  $\mu\text{m}$ ) of SiC were added in the matrix as particulate fillers. Figure 1 shows the scanning electron microscopy (SEM) images for the components.

In the specimen fabrication, UHMWPE powder and SiC fillers were distributed in an ethanol medium to obtain a homogenous mixture. After a 20 min blending process, the mixtures were rested at 79 °C in an oven to evaporate the ethanol. The dried mixtures were subjected to a compression molding chamber in a Struers CitoPress-1 machine to produce bulk composites. Molding temperature was fixed at 150 °C because the melting point of UHMWPE is around 136 °C [22, 23]. It is suggested that molding operation is completed just above the melting point of polymers to avoid decomposition in the polymer while ensuring a fully melted microstructure [24]. Molding pressure was varied in three levels, such as 50, 200 and 350 bar, and thereby investigating its effects on the machining properties of the composites. Furthermore, the amount and size of SiC additives were

changed in the specimen fabrication stage to investigate the influences of these two parameters in the experiments.

In the micro-machining tests, the composites were machined in dry conditions using a flat, micro-end cutter having eight flutes. Feed rate and axial depth of cut were used as constant, such as 100 mm/min and 200  $\mu\text{m}$ , respectively. For each case, the tests were completed by opening three slots on the specimens. Figure 2 shows the details of the specimens and cutter. Table 1 gives the design of the specimens, which were machined at three different spindle speeds: 8000, 16,000 and 28,000 rpm in the experiments.

### 2.2 Measurement equipment and techniques

Surface roughness measurements were carried out with a Mitutoyo SJ-400 surface profilometer. Scanning electron

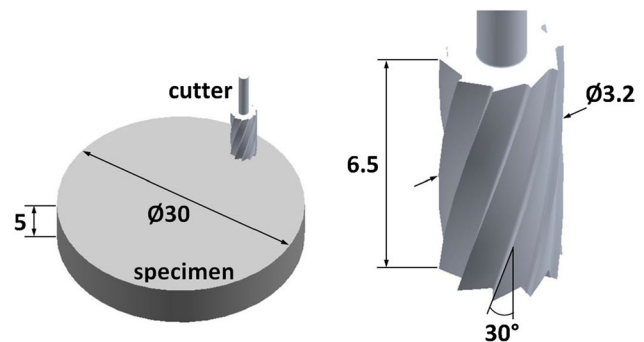
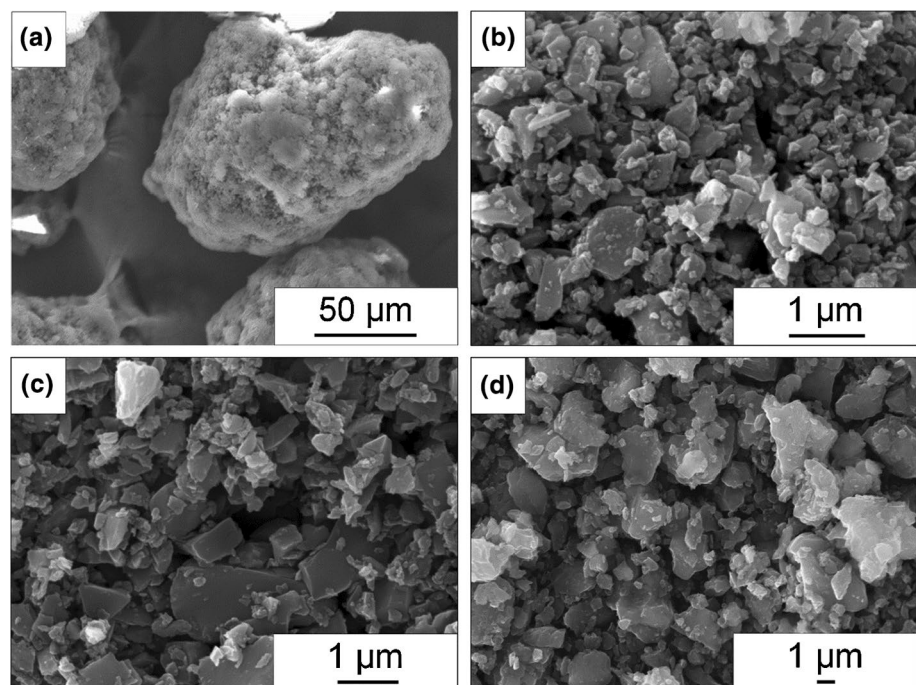


Fig. 2 Details of the specimens and cutter (dimensions in mm)

Fig. 1 SEM images for **a** UHMWPE, **b** 0.3  $\mu\text{m}$  SiC, **c** 0.5  $\mu\text{m}$  SiC and **d** 1.0  $\mu\text{m}$  SiC



**Table 1** Design of the specimens

Specimen code	Molding pressure (bar)	Filler loading (wt%)	Filler size ( $\mu\text{m}$ )
1	350	0	–
2	350	2	1.0
3	350	5	1.0
4	350	10	1.0
5	200	10	1.0
6	50	10	1.0
7	350	10	0.5
8	350	10	0.3

microscopy (SEM) and energy-dispersive spectrometry (EDS) analyses were conducted with a Hitachi Regulus 8230 system. Cutting temperatures were displayed using an Optris PI400 thermography system.

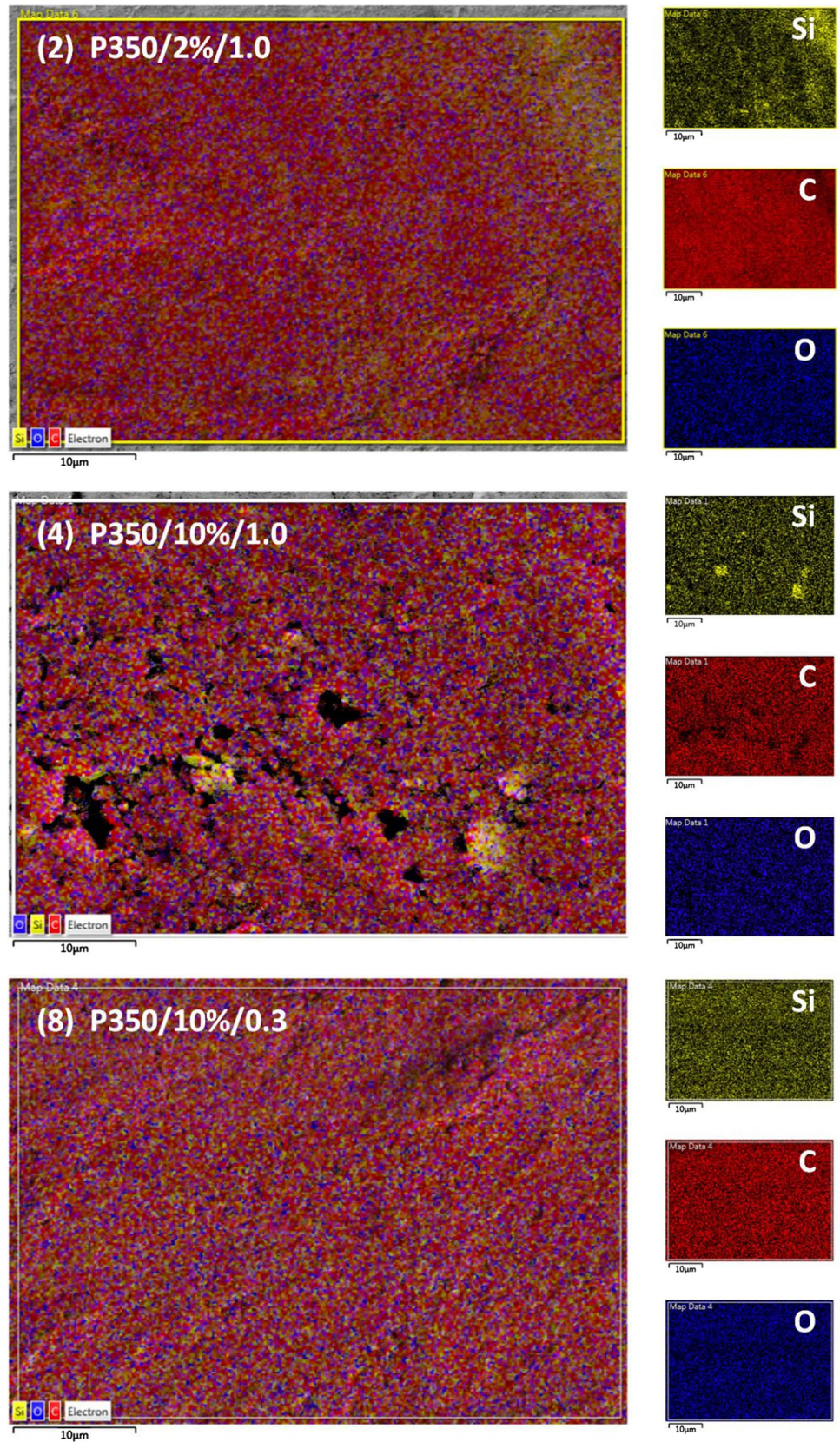
### 3 Results and discussion

Figure 3 shows the EDS mapping images for 2, 4 and 8 coded specimens to identify the effects of filler amount and size in the polymeric matrix. In the images, silicon (Si) element corresponds to the presence of SiC in the matrix. Comparing the images for the specimens with 2 and 4 codes, SiC fillers exhibit a denser distribution in specimen 4 due to the increased filler loading. On the other hand, Si density is slightly higher in specimen 8 than that in specimen 4, although the filler amounts are identical with each other. This arises from the particle size of carbide fillers because fillers with fine particles include a higher number of particles with respect to coarse ones even if the loading rate is the same as each other. Figure 4 shows the surface roughness results measured from the milling channels for each specimen. Considering the effect of spindle speed, it is clear that surface roughness reduces by increasing spindle speed in the milling operations. This trend is also consistent with previous studies [25, 26] that at high spindle speeds, thrust force reduces in the cutting process and thereby leading to a smoother surface finishing as such in metal cutting operations. Differently from metal cutting, material melting at cutting zone may be observed in polymer machining operations due to low melting points of polymers. After local melting at cutting zone, material surface solidifies while cutter provides the ironing effect for this surface and therefore, a smoother surface is achieved. As shown in the thermography images in Fig. 12 in “Appendix”, cutting temperatures exceed the melting point of UHMWPE, especially in the operations at 28,000 rpm for the composites consolidated with 10wt% fillers. Filler amount has a negative effect on the surface roughness results, although carbide particles

enhance the cutting temperature during the process. Carbide fillers lead to severe frictional interactions during cutting and consequently increasing the heat generation in the process. Carbide particles act as rigid anchors within the UHMWPE matrix and they cause higher forces to shear the polymer matrix. In addition, cutter surfaces are subjected to harsh interaction with hard fillers within the UHMWPE matrix. Another reason for increased surface roughness at high filler amounts is a protrusion of carbide particles from the specimen surfaces. Although polymer matrix provides smoother surface finishes in high spindle speed processes, carbide particles result in increased surface roughness due to hard asperities on the composite surfaces. Figure 5 shows the SEM images for the specimens, including different filler amounts. The thermal effect is also obvious on the surfaces that polymer matrices show lamellar topographies smearing along the cutting direction, especially at high filler amounts and high spindle speeds.

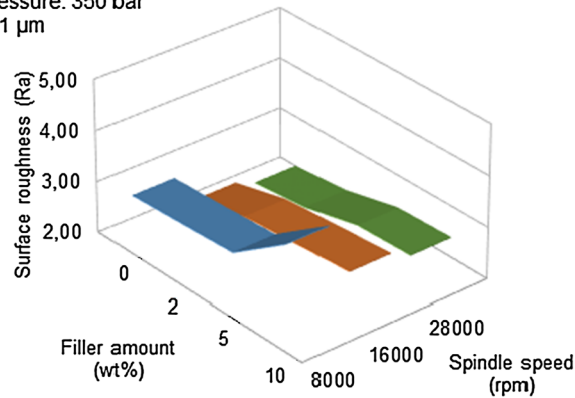
Considering the surface roughness results given in Fig. 4c, it is possible to mention that filler size is important in low spindle speed operations, however, the impact of filler size gradually reduces by increasing spindle speed in the milling operation. At 28,000 rpm, the surface roughness results are in a very narrow band from Ra 2.58 to 2.62 for the carbide size of 1.0–0.3  $\mu\text{m}$ . Finer size carbides provide larger filler/matrix interfaces due to their larger surface areas and thereby resulting in a stronger interaction between carbide particles and the UHMWPE matrix. For this reason, the machinability of the composites gets difficult, which requires higher forces for material removal. Hence, polymers with fine fillers produce poorer surface finish after machining in comparison to polymers with coarse ones. However, this effect gradually diminishes as spindle speed increases in the process because high deformation rates are highly sufficient for smoother cutting operations. Figure 6 shows the SEM images for the specimens, including different filler sizes. From these images, lamellar surface characteristics are predominant due to the thermal softening and melting of the polymer matrices. As cutting temperature increases in the process, ductile elongations become more visible in the microstructures as such in the specimens 7 and 8 machined at 8000 rpm. At the same filler amounts, fine fillers have an increased number of particles with respect to coarse fillers. For this reason, fine fillers exhibit denser distributions than coarse fillers in the polymer matrix, as shown in Fig. 3. Hence, the anchoring effect in fine size carbides gets stronger within the polymer matrix and therefore, material removal grows difficult due to higher consolidation. Because of this fact, high elongations of the UHMWPE matrix around the carbide particles are observed during cutting. The cutting mechanism turns into the tearing of layers from the material. Hence, specimen surfaces exhibit excessive deformations, which result in increased surface roughness after the

**Fig. 3** EDS mapping for the specimens

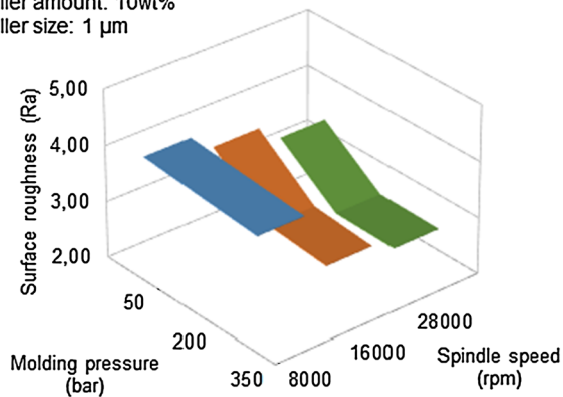


**(a) Constants**

Molding pressure: 350 bar  
 Filler size: 1  $\mu\text{m}$

**(b)****Constants**

Filler amount: 10wt%  
 Filler size: 1  $\mu\text{m}$

**(c)****Constants**

Molding pressure: 350 bar  
 Filler amount: 10wt%

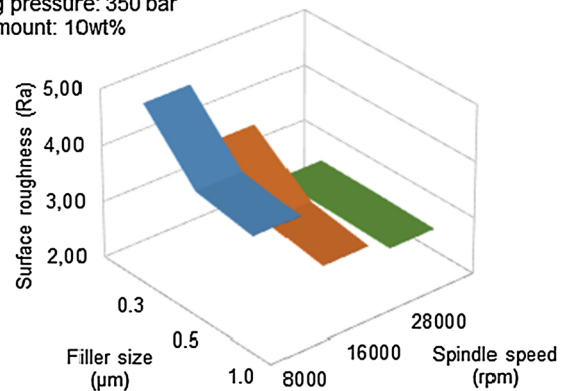


**Fig. 4** Surface roughness with respect to **a** filler amount, **b** molding pressure and **c** filler size

operation. On the other hand, at 28,000 rpm, plastic flows are shown on a small scale like small ridges or lamellas on the specimen surfaces. Because cutting temperatures are excessive such as  $> 148\text{ }^{\circ}\text{C}$  in these operations, UHMWPE matrices are more likely to melt locally in cutting zone and thereby reducing the cutting forces. For this reason, the cutting process is facilitated by thermal effect as well as providing lower surface roughness on the specimens. Due to this mechanism, cutting channels show small plastic flow patterns after the machining operations.

To achieve a successful molding process for UHMWPE, two successive stages have to be completed adequately [24]. The first stage is related to heating of polymer powder above the melting point while applying a sufficient compression to the powder bulk. Under these conditions, polymer particles physically touch each other and therefore, molecular interactions between the particles are increased in the polymer melt. Voids are eliminated from the medium by the effect of compression. In the second stage, molecular contacts turn into molecular bonds due to continuous diffusion in

the polymer melt. Molecular bonds are established at some chain ends. However, the bonding process is extended to the whole body as the diffusion runs for a while. The molecular bonding process results in completely entangled chains by removing the particle boundaries within the polymer bulk, which means that contacted polymer particles form a continuous structure with fully knitted molecular chains [27]. In this light, it is possible to mention that molding pressure is profoundly crucial for the molecular structure of the molded specimens because higher pressures increase the number of particle contacts in the first stage and thereby facilitating the diffusion process in the second stage. For this reason, specimens molded at higher pressures exhibit improved microstructural consolidation, as stated in previous studies [28–30]. Considering the surface roughness results in Fig. 4b, specimens molded at higher pressures provide improved surface finish after machining. However, this effect comes into prominence in the high spindle speed operations, such as those at 16,000 and 28,000 rpm. At 8000 rpm, there is almost no variation in the surface roughness results with

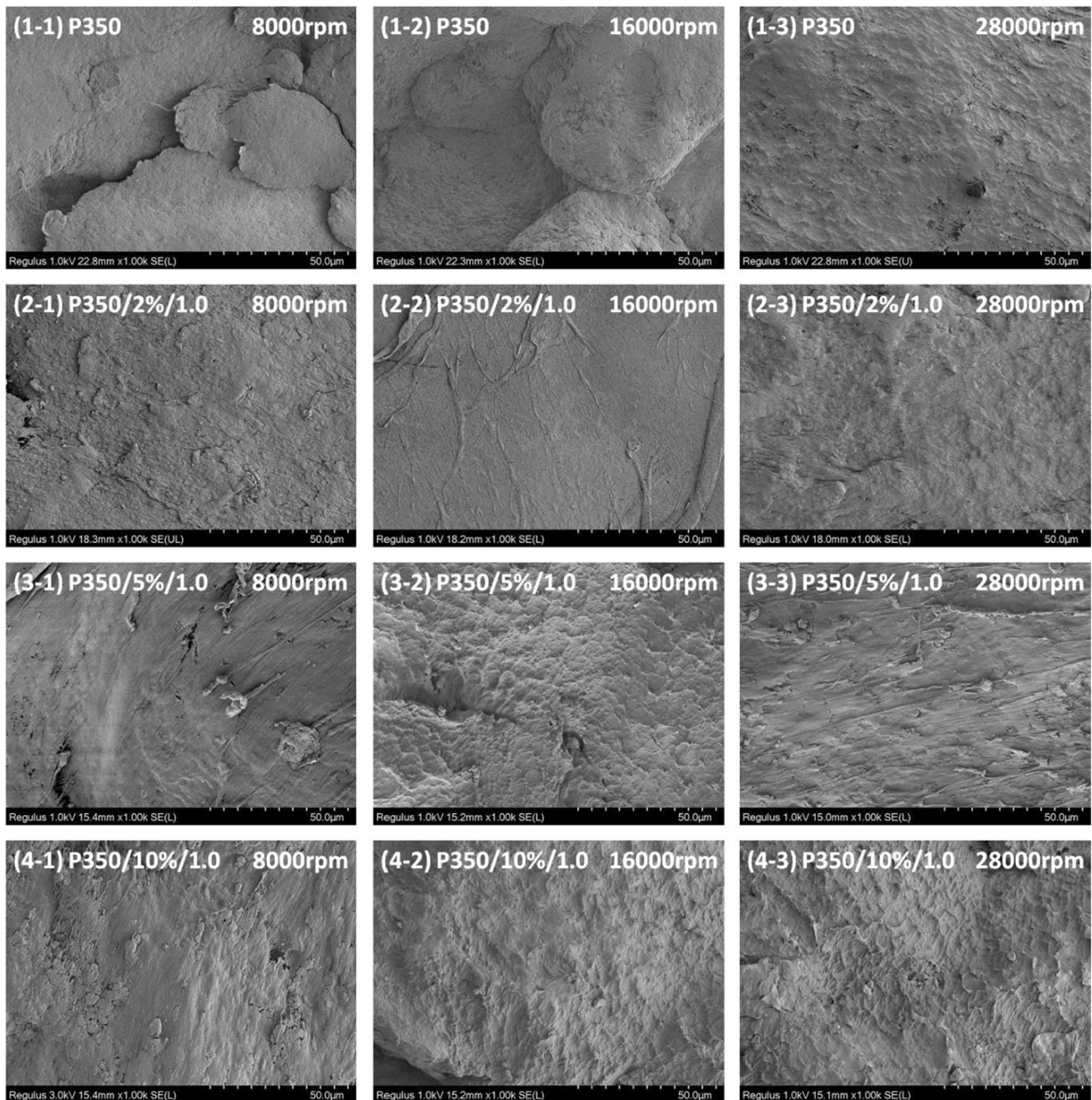


**Fig. 5** SEM images for the specimens including different filler amounts

respect to molding pressure. From the results, roughness values are Ra 4.01, 3.92 and 3.84 for the specimens with 10wt% of carbide fillers having 0.3, 0.5 and 1.0  $\mu\text{m}$ , respectively. At low spindle speeds, the cutter is more prone to tearing of chips from the specimens rather than a pure shearing and thereby resulting in poor surface finishes regardless of a pressure effect. This is associated with that cross-linked polymers are lack of deforming or flowing over long distances and thus, they are ruptured or torn during material

removal processes [31]. Figure 7 shows the chip morphologies produced from specimen 4 after the machining operations at different spindle speeds. As shown in these images, there is an irregular shape with material elongations, which correspond to tearing or rupturing in the cutting operation at 8000 rpm. However, at 16,000 and 28,000 rpm, the chips are helical and continuous, which means there is an easy chip flow in the cutting operations. Surface roughness gets lower values at high spindle speeds, however, it is important to

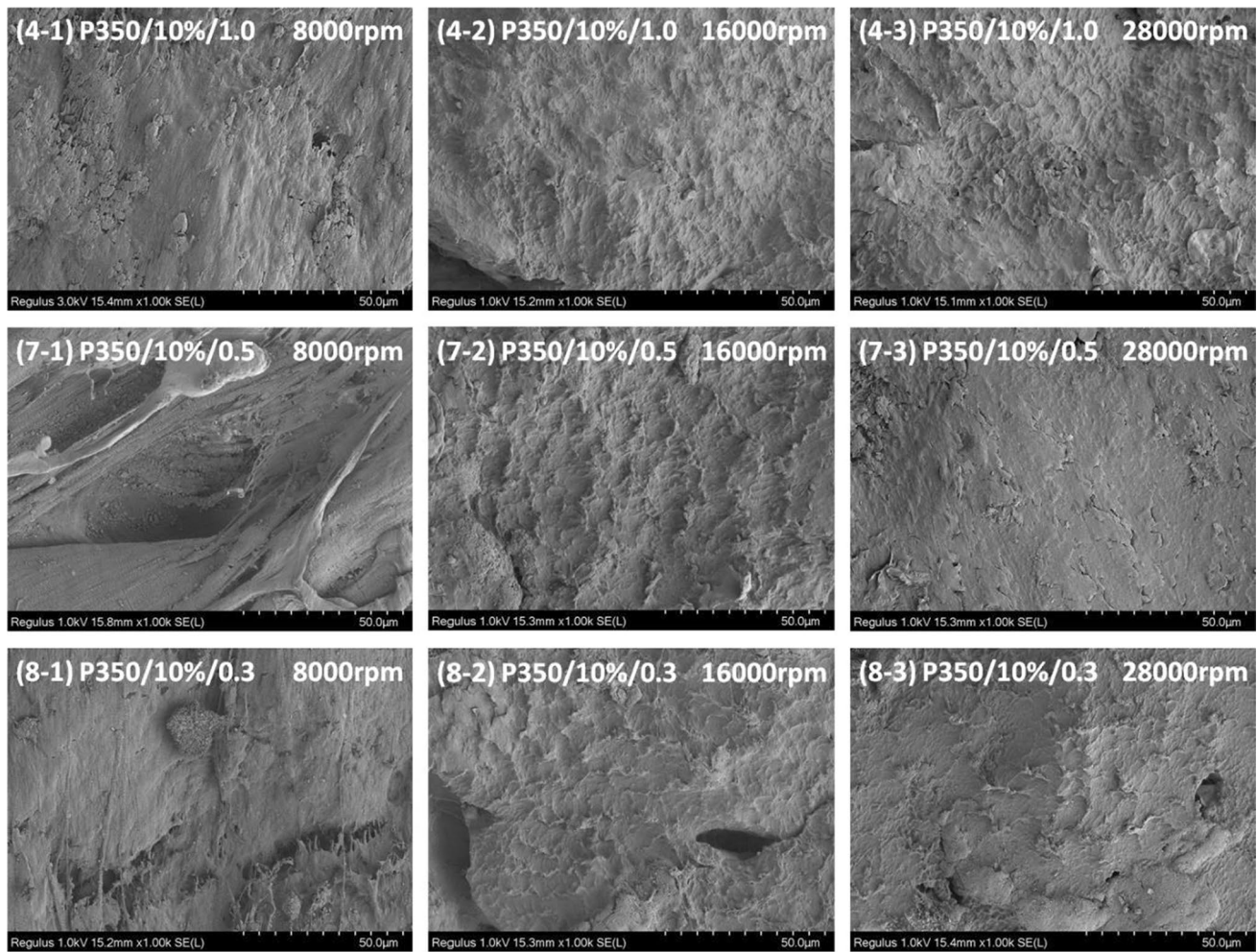


**Fig. 6** SEM images for the specimens including different filler sizes

note that there is a drastic reduction in the surface roughness results when the specimens change from 50 bar molding to 200 bar molding in the 16,000 and 28,000 rpm machining operations (Fig. 4b). Despite this significant fall, the specimens molded at 200 and 350 bar exhibit almost identical surface finishes for the 16,000 and 28,000 rpm cutting operations. As stated by Wang et al. [32], UHMWPE hardness exhibits an increase by increasing molding pressure; however, this improvement in the polymer hardness becomes negligible beyond 150 bar. For this reason, the specimens molded at 200 and 350 bar show close surface qualities after machining. It is also important to note that carbide fillers are packed tightly in the specimens molded at higher pressures, which results in improved microstructural consolidation. Hence, the detachment of particulate fillers from the machined surface is suppressed and therefore, surface quality is improved using higher pressures in the molding stage. Figure 8 shows the SEM images for the specimens molded at different pressures. It is shown that the machined

surfaces for the specimen molded at 50 bar include torn or ruptured debris, especially in the machining operation at 8000 and 16,000 rpm. These debris are hardly visible due to the increased cutting temperatures using the spindle speed of 28,000 rpm.

Figure 9 shows the maximum cutting temperatures with respect to different parameters, such as spindle speed, molding pressure, filler amount and filler size. From these results, there are some systematic variations in the cutting temperatures, which are associated with heat generation in the machining operation. Regarding the spindle speed, all charts in Fig. 9 show that higher spindle speeds lead to higher cutting temperatures in the machining zone. This trend can be explained by the increased dissipated energy through plastic deformation and friction in the cutting zone. For this reason, increased heat generation results in excessive cutting temperatures at high spindle speeds [33–35]. In metal cutting, heat generation can be dissipated over a large volume due to the higher thermal conductivity of metals. However,



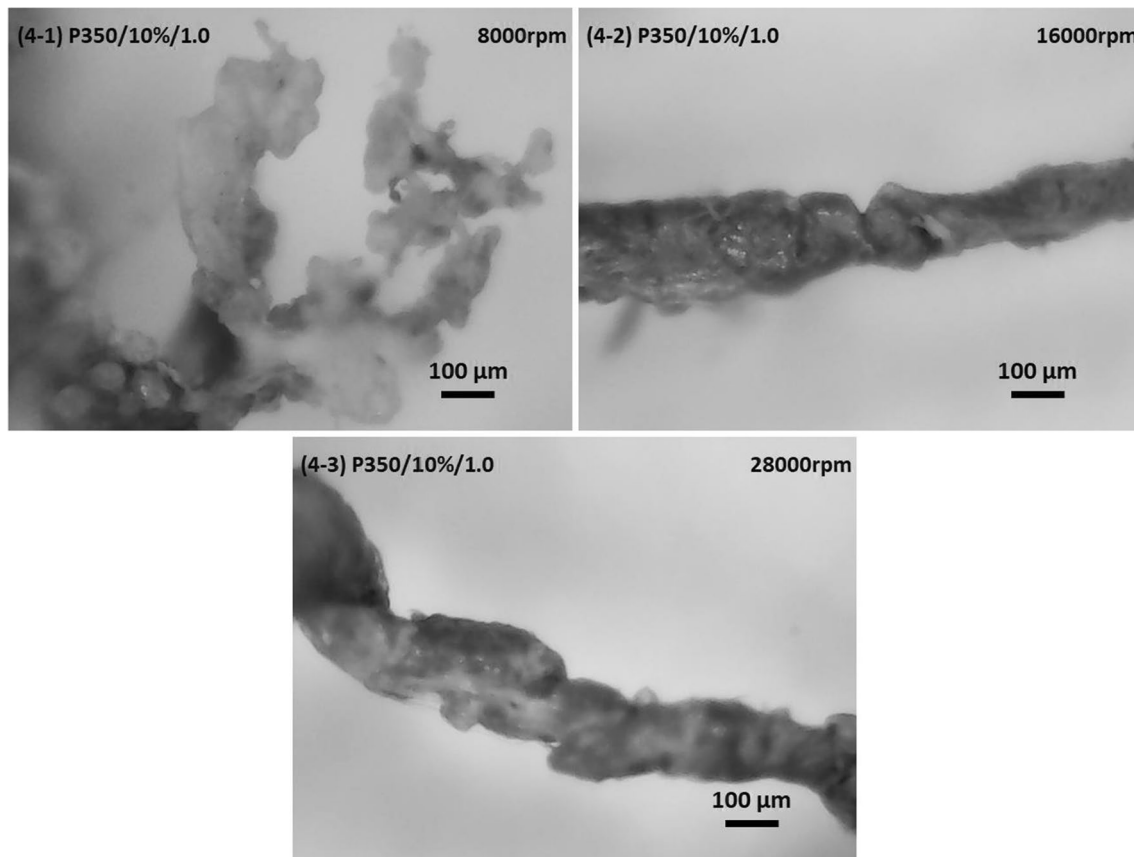


**Fig. 7** Chip morphologies in the machining operations at different spindle speeds

polymers have poor thermal conductivity, which leads to heat accumulation in a local area during cutting. According to the manufacturers' specifications, UHMWPE has a thermal conductivity range of 0.42–0.51 W/mK, which is nearly five-100-fold lower than that for aluminum. It is possible to mention that heat accumulation results in the local melting of the specimens, especially in the high spindle speed operations, where cutting temperatures are above the melting point of UHMWPE. Considering the effect of filler amount in Fig. 9a, cutting temperatures show an increasing trend by including more carbide fillers in the UHMWPE matrix regardless of spindle speed. Although the results are in a close band up to 5 wt% carbide loadings, the jumps in the cutting temperatures are drastic for the specimens consolidated with 10 wt% fillers. Despite relatively higher thermal conductivity of SiC particles (140–120 W/mK for the range of 20–150 °C [36]), the carbide reinforced specimens exhibit higher temperatures than the neat specimens during machining. Higher cutting temperatures arise from the increased frictional interactions in the polymers, including fillers. During cutting operation, hard carbide particles cannot be deformed plastically in the soft polymer medium and therefore, these particles are pushed and stirred in the thermally

softened or melted polymer pool. During this process, filler/matrix interfaces result in high frictional effects, which generate excessive heat in the cutting zone. Also, carbide particles lead to an abrasive effect on the cutter surfaces, which is an additional heat generation mechanism in the SiC included specimens. For this reason, cutting temperature increases by including more particles in the polymer matrix, especially above the loading rate of 5 wt%. Figure 9c shows the relationship between cutting temperature and filler size for the operations conducted at different spindle speeds. From this chart, it is obvious that there is a suppression in the cutting temperatures using coarser carbide particles in the UHMWPE matrix. This trend is attributed to the increased number of carbide particles using fine size fillers. Smaller size particles exhibit denser distribution in the polymer matrix and therefore, frictional interactions are enhanced due to larger surface area of filler phase in the composite. In addition, this effect increases the contact points between fillers and cutter surfaces. Considering Fig. 9b, specimens molded at higher pressures show higher cutting temperatures during machining. This is related to the consolidation of microstructure, which gets stronger at higher molding pressures. As stated by Wu et al. [27], particle contacts in

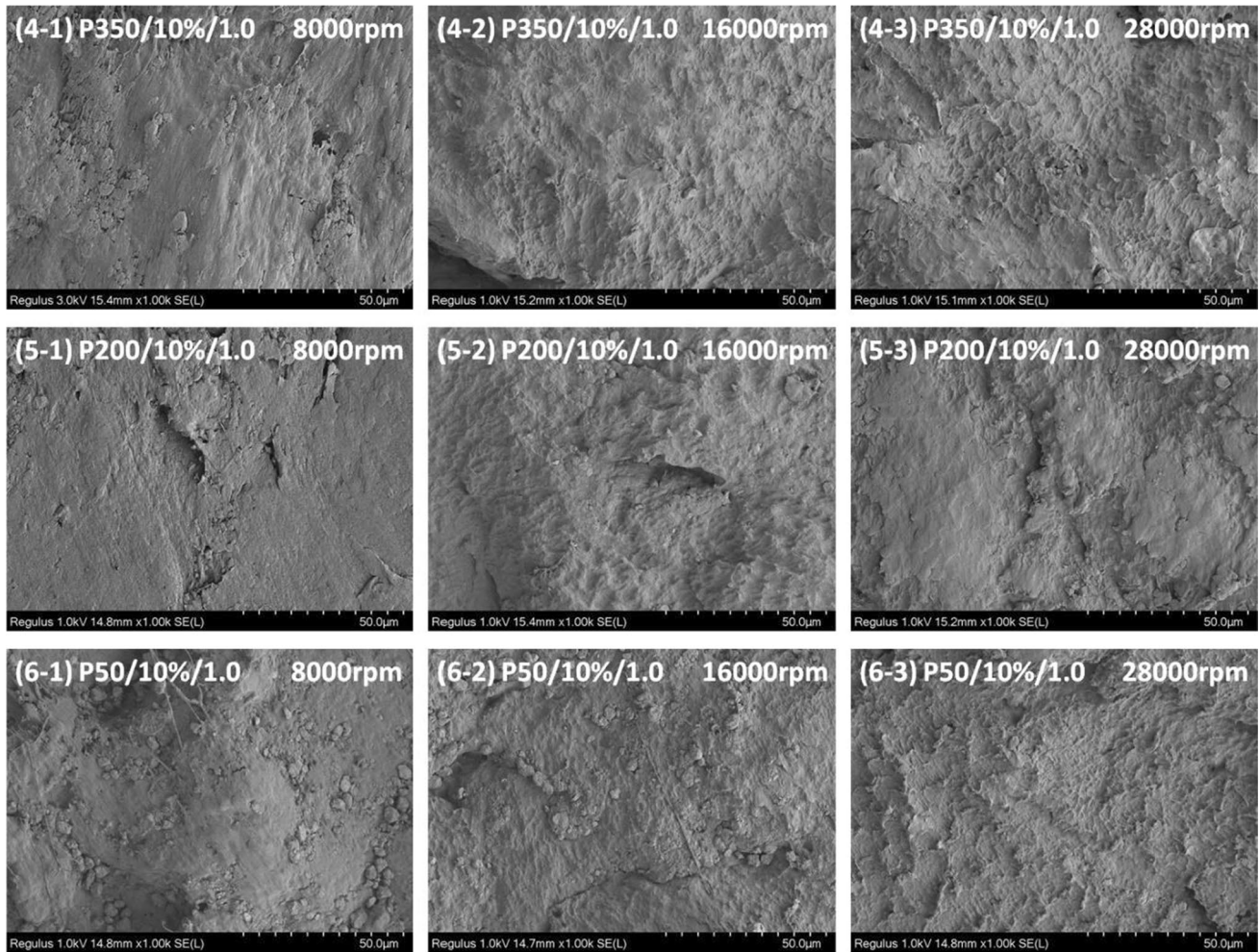


**Fig. 8** SEM images for the specimens molded at different pressures

the powdered polymer are increased by the effect of higher molding pressure and heating this bulk, molecular bonding is initiated due to the diffusion process. For this reason, higher pressure in the molding stage leads to an increased number of particle contacts and thereby facilitating the diffusion process, which results in a highly entangled molecular bonding within the material. Hence, strong and entangled molecular bonds provide microstructural consolidation and thus, material removal becomes difficult where the shearing process results in higher cutting temperatures.

To evaluate the relationship between the inputs and responses, non-linear regression analysis was carried out based on 24 data, as given in Table 2. From the analyses, the determination coefficient of the regression model,  $R^2$  is 0.89 and 0.94 for surface roughness and cutting temperature, respectively. Also, the adjusted determination coefficient of the regression model, adjusted  $R^2$  is 0.83 and 0.91 for surface roughness and cutting temperature, respectively. Hence, it is possible to mention that the regression models are able

to capture most of the relationships between the responses and the inputs because determination coefficients are higher than the limit of 0.80. Tables 3 and 4 show the analysis of variance (ANOVA) results to specify both reactive and non-reactive effects of experimental parameter reactions. From the ANOVA analyses, the results satisfy the reliability interval of 95% by considering the significance level, which is lower than 5% ( $p \leq 0.05$ ). Equation 1 and Eq. 2 give the regression models for surface roughness and cutting temperature, respectively. Regarding the surface roughness ( $Y_1$ ) model, it is seen that molding pressure ( $X_1$ ), filler size ( $X_3$ ) and spindle speed ( $X_4$ ) show inverse proportionality. However, surface roughness ( $Y_1$ ) shows an increasing relationship with increasing filler loading ( $X_2$ ). Figure 10 shows the contribution of variables to the surface roughness results in terms of SS values from ANOVA. From this chart, spindle speed ( $X_4$ ) has the highest impact on the surface roughness. On the other hand, the only negative relationship in the cutting temperature ( $Y_2$ ) model is with filler size ( $X_3$ ). However,

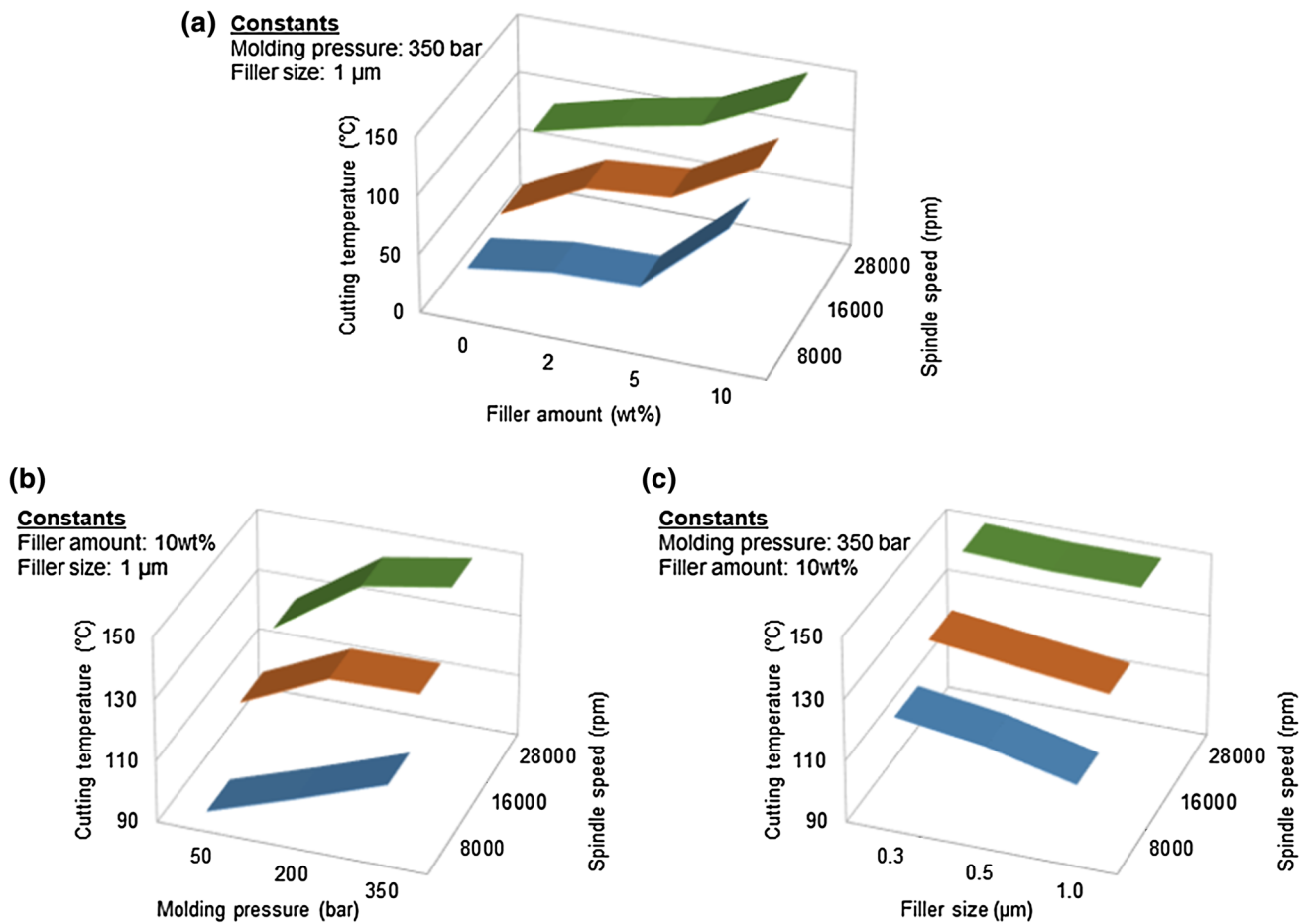


Fig. 9 Maximum cutting temperatures with respect to a filler amount, b molding pressure and c filler size

cutting temperature ( $Y_2$ ) shows an increasing relationship with increasing molding pressure ( $X_1$ ), filler loading ( $X_2$ ) and spindle speed ( $X_4$ ). According to the contribution of variables to cutting temperature as given in Fig. 11, filler loading ( $X_2$ ) has the highest impact while spindle speed ( $X_4$ ) is the next input having considerable influence on cutting temperature. Conversely, molding pressure ( $X_1$ ) and filler size ( $X_3$ ) have relatively lower effects on the rising of cutting temperature during the machining operation. For both models, interaction effects are not significant considering their P-levels in ANOVA results (Tables 3, 4),

$$\begin{aligned}
 Y_1 = & 2.66 - 0.127X_1 + 1.28X_2 - 0.067X_3 - 0.023X_4 \\
 & - 0.105X_1X_4 - 0.185X_2X_3 - 0.191X_2X_4 + 0.123X_3X_4 \\
 (S = & 0.297626 \text{ R - Sq} = 88.6\% \text{ R - Sq (adj)} = 82.5\%),
 \end{aligned}
 \tag{1}$$

$$\begin{aligned}
 Y_2 = & -24.1 + 4.47X_1 + 39.2X_2 - 14.2X_3 \\
 & + 20.2X_4 + 0.76X_1X_4 + 0.004X_2X_3 \\
 & - 6.04X_2X_4 + 4.99X_3X_4 \\
 (S = & 10.1437 \text{ R - Sq} = 94.1\% \text{ R - Sq (adj)} = 90.9\%).
 \end{aligned}
 \tag{2}$$

### 4 Conclusion

In the present work, micro-milling operations were carried out for newly developed ceramic reinforced polymer composite materials. The composites were molded from the mixture of powdered UHMWPE and particulate carbide fillers. To investigate the effects of material based parameters on the machining results, molding pressure, filler amount and filler size were varied in the molding stage. In addition, various spindle speeds were used while feed rate and cutting depth were kept constant in the machining operations. The outputs of cutting temperature and surface

**Table 2** Inputs and responses in the regression analyses

$X_1$	$X_2$	$X_3$	$X_4$	$Y_1$	$Y_2$
3	1	1	1	2.95	39.4
3	2	4	1	3.00	49.6
3	3	4	1	3.06	51.6
3	4	4	1	3.84	113.8
2	4	4	1	3.92	103.5
1	4	4	1	4.02	93.8
3	4	3	1	4.01	120.7
3	4	2	1	5.09	124.8
3	1	1	2	2.35	48.4
3	2	4	2	2.63	83.8
3	3	4	2	2.71	89.4
3	4	4	2	2.79	128.2
2	4	4	2	2.89	127.7
1	4	4	2	3.70	114.7
3	4	3	3	2.97	131.6
3	4	2	3	3.77	135.2
3	1	1	3	2.19	83.6
3	2	4	3	2.30	101.1
3	3	4	3	2.55	114.9
3	4	4	3	2.58	148.4
2	4	4	3	2.60	143.7
1	4	4	3	3.37	124.8
3	4	3	3	2.61	148.5
3	4	2	3	2.62	152.0

$X_1$  is the Molding pressure: 50, 200, 350 bar (levels: 1, 2, 3)

$X_2$  is the Filler loading: 0, 2, 5, 10wt% (levels: 1, 2, 3, 4)

$X_3$ : Filler size: 0, 0.3, 0.5, 1  $\mu\text{m}$  (levels: 1, 2, 3, 4)

$X_4$  is the Spindle speed: 8000, 16,000, 28,000 rpm (levels: 1, 2, 3)

$Y_1$  is the Surface roughness (Ra)

$Y_2$  is the Cutting temperature ( $^{\circ}\text{C}$ )

**Table 3** ANOVA results for surface roughness

Source	$df$	SS	MS	$F$	$p$
Regression	8	10.2953	1.2869	14.53	<0.05
$X_1$	1	1.1429	1.1429	12.90	<0.05
$X_2$	1	2.0644	2.0644	23.30	<0.05
$X_3$	1	0.7764	0.7764	8.76	<0.05
$X_4$	1	4.8615	4.8615	54.87	<0.05
$X_1X_4$	1	0.0374	0.0374	0.42	>0.05
$X_2X_3$	1	0.7863	0.7863	8.87	<0.05
$X_2X_4$	1	0.3978	0.3978	4.49	>0.05
$X_3X_4$	1	0.2287	0.2287	2.58	>0.05
Error	15	1.3287	0.0886		
Total	23	11.6240			

**Table 4** ANOVA results for cutting temperature

Source	$df$	SS	MS	$F$	$p$
Regression	8	24,515.7	3064.5	29.78	0.000
$X_1$	1	504.1	504.1	4.90	<0.05
$X_2$	1	16,995.9	16,995.9	165.17	<0.05
$X_3$	1	533.6	533.6	5.18	<0.05
$X_4$	1	5751.1	5751.1	55.9	<0.05
$X_1X_4$	1	5.6	5.6	0.05	>0.05
$X_2X_3$	1	8.9	8.9	0.09	>0.05
$X_2X_4$	1	337.7	337.7	3.28	>0.05
$X_3X_4$	1	378.8	378.8	3.68	>0.05
Error	15	1543.4	102.9		
Total	23	26,059.1			

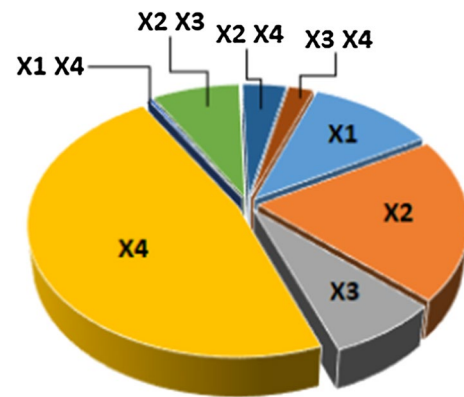


**Fig. 10** Contribution of variables in terms of SS values (surface roughness)

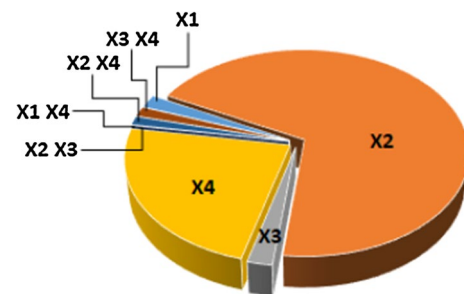


**Fig. 11** Contribution of variables in terms of SS values (cutting temperature)

roughness were considered in the results. Moreover, chip morphology and machined surfaces were analyzed using scanning electron microscopy. To evaluate the relationships between the process parameters, regression analyses were carried out based on the experimental data. According to the results, the following conclusions can be drawn:

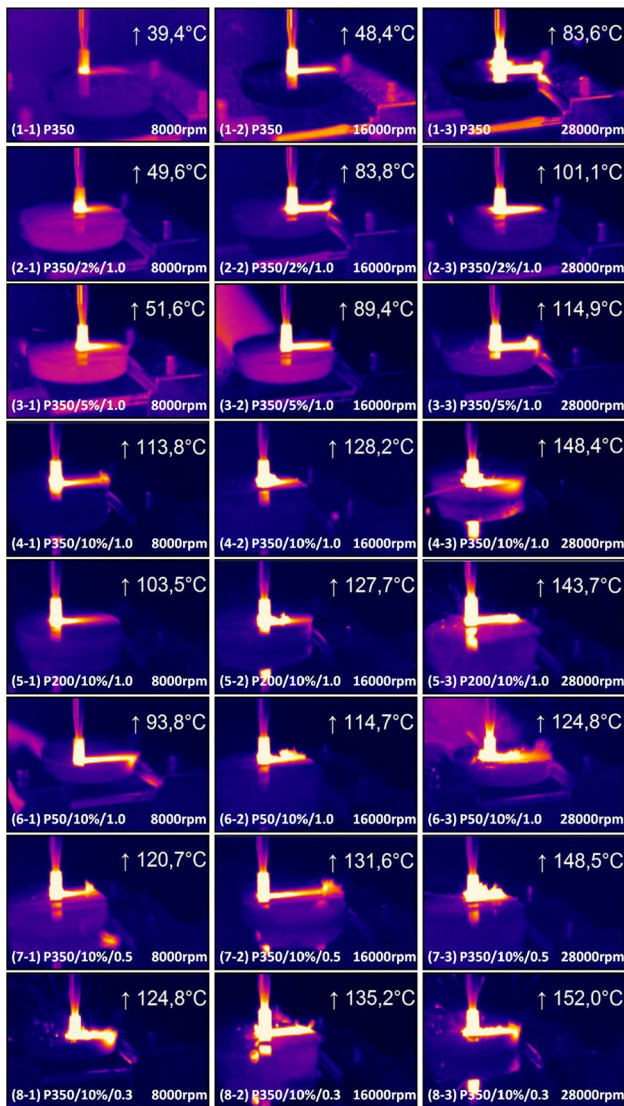


Fig. 12 Thermography images for each specimen

- Surface roughness reduces by increasing spindle speed because material removal is realized through tearing or rupturing mechanisms at low speeds while shearing develops in high speed operations.
- Specimens produced at higher molding pressures exhibit smoother surface finishes after machining operations however, this trend is pronounced at high spindle speeds.
- Higher filler amounts in the composites lead to lower surface qualities after milling operations however, this effect is suppressed at high spindle speeds.
- Composites with coarser fillers reduce surface roughness after machining however, filler size effect fades away at high spindle speeds.
- UHMWPE matrix may exhibit local melting rather than thermal softening in cutting zone. Matrix melt-

ing is more likely to develop at high filler loadings and high spindle speeds.

- Composites molded at higher pressures lead to higher cutting temperatures during machining operations because higher molding pressures enhances the microstructural consolidation that requires higher energy for material removal.
- Cutting temperatures are lowered using coarser fillers in the composites however, filler size effect is important in low spindle speed operations.
- Lamellar surface morphology is predominant after machining because thermal softening and/or melting of the polymer matrix create wavy formations in cutting zone.
- Chips exhibit irregular shapes at low spindle speeds due to predominant tearing mechanisms in machining operations. However, shearing mechanism prevails over tearing at higher speeds and chip formation turns into helical and continuous phase.

This work mainly focusses on the effects of material variables (molding pressure, filler amount and filler size) in micro-milling operations rather than the machining parameters. To investigate the machining characteristics of hard filler reinforced polymer composites, the role of machining parameters will be studied in the future works.

## Appendix

Full set of thermography images are given in Fig. 12.

**Acknowledgements** The authors gratefully acknowledge the financial support by the Research Fund of Eskişehir Osmangazi University, Project #202015046.

**Author contributions** Conceptualization: SG; methodology: SG; writing—reviewing and editing: SG; investigation: MAS, data curation: MAS; software: MAS.

**Funding** Research Fund of Eskişehir Osmangazi University, Project #202015046.

## Declarations

**Conflict of interest** All authors declare that they have no conflict of interest.

**Availability of data and material** The raw/processed data required to reproduce these findings cannot be shared at this time as the data also forms part of an ongoing study.

**Code availability** Not applicable.

## References

- Jiang Z, Zhao J, Xie H. Microforming technology: theory, simulation and practice. London: Academic Press; 2017.
- Koç M (2020) Micro-manufacturing: design and manufacturing of micro-products. Hoboken: Wiley; 2011. <https://www.myilibrary.com/?id=305245>. Accessed 19 Mar 2020 (Online).
- Razali AR, Qin Y. A review on micro-manufacturing, micro-forming and their key issues. *Procedia Eng.* 2013;53:665–72. <https://doi.org/10.1016/j.proeng.2013.02.086>.
- Ratchev S, International Federation for Information Processing, (editors). Precision assembly technologies and systems: 5th IFIP Wg 5.5 International precision assembly seminar, proceedings. Chamonix, Berlin: IPAS 2010, Springer; 2010.
- Qin Y, et al. Development of a new machine system for the forming of micro-sheet-products. *Int J Mater Form.* 2008;1(S1):475–8. <https://doi.org/10.1007/s12289-008-0098-9>.
- Sharma AK, Bhandari R, Aherwar A, Rimašauskienė R. Matrix materials used in composites: a comprehensive study. *Mater Today Proc.* 2020;21:1559–62. <https://doi.org/10.1016/j.matpr.2019.11.086>.
- Kumar R, Singh S, Sidhu AS, Pruncu CI. Bibliometric analysis of specific energy consumption (SEC) in machining operations: a sustainable response. *Sustainability.* 2021;13(10):5617. <https://doi.org/10.3390/su13105617>.
- Ahmad J. Machining of polymer composites. Boston: Springer; 2009. <https://doi.org/10.1007/978-0-387-68619-6>.
- Hocheng H, editor. Machining technology for composite materials: principles and practice. Cambridge, Philadelphia: Woodhead Publishing; 2012.
- Sheikh-Ahmad J, Twomey J, Kalla D, Lodhia P. Multiple regression and committee neural network force prediction models in milling FRP. *Mach Sci Technol.* 2007;11(3):391–412. <https://doi.org/10.1080/10910340701554873>.
- Gara S, Tsoumarev O. Effect of tool geometry on surface roughness in slotting of CFRP. *Int J Adv Manuf Technol.* 2016;86(1–4):451–61. <https://doi.org/10.1007/s00170-015-8185-9>.
- Gara S, M'hamed S, Tsoumarev O. Temperature measurement and machining damage in slotting of multidirectional CFRP laminate. *Mach Sci Technol.* 2018;22(2):320–37. <https://doi.org/10.1080/10910344.2017.1365892>.
- Azmi AI, Lin RJT, Bhattacharyya D. Machinability study of glass fibre-reinforced polymer composites during end milling. *Int J Adv Manuf Technol.* 2013;64(1–4):247–61. <https://doi.org/10.1007/s00170-012-4006-6>.
- Ghafarizadeh S, Chatelain J-F, Lebrun G. Finite element analysis of surface milling of carbon fiber-reinforced composites. *Int J Adv Manuf Technol.* 2016;87(1–4):399–409. <https://doi.org/10.1007/s00170-016-8482-y>.
- He Y, Qing H, Zhang S, Wang D, Zhu S. The cutting force and defect analysis in milling of carbon fiber-reinforced polymer (CFRP) composite. *Int J Adv Manuf Technol.* 2017;93(5–8):1829–42. <https://doi.org/10.1007/s00170-017-0613-6>.
- Pecat O, Rentsch R, Brinksmeier E. Influence of milling process parameters on the surface integrity of CFRP. *Procedia CIRP.* 2012;1:466–70. <https://doi.org/10.1016/j.procir.2012.04.083>.
- Iskandar Y, Tendolkar A, Attia MH, Hendrick P, Damir A, Diakodimitris C. Flow visualization and characterization for optimized MQL machining of composites. *CIRP Ann.* 2014;63(1):77–80. <https://doi.org/10.1016/j.cirp.2014.03.078>.
- Hintze W, Hartmann D. Modeling of delamination during milling of unidirectional CFRP. *Procedia CIRP.* 2013;8:444–9. <https://doi.org/10.1016/j.procir.2013.06.131>.
- Szallies K, Siebert N, Bergmann JP. Low frequency oscillated milling of carbon fiber-reinforced plastics. *Procedia CIRP.* 2017;66:153–8. <https://doi.org/10.1016/j.procir.2017.03.298>.
- Mishra TK, Kumar A, Verma V, Pandey KN, Kumar V. PEEK composites reinforced with zirconia nanofiller. *Compos Sci Technol.* 2012;72(13):1627–31. <https://doi.org/10.1016/j.compscitech.2012.06.019>.
- Agrawal A, Satapathy A. Thermal and dielectric behaviour of polypropylene composites reinforced with ceramic fillers. *J Mater Sci Mater Electron.* 2015;26(1):103–12. <https://doi.org/10.1007/s10854-014-2370-8>.
- Ge S, et al. Friction and wear behavior of nitrogen ion implanted UHMWPE against ZrO<sub>2</sub> ceramic. *Wear.* 2003;255(7–12):1069–75. [https://doi.org/10.1016/S0043-1648\(03\)00269-2](https://doi.org/10.1016/S0043-1648(03)00269-2).
- Xiong D, Ge S. Friction and wear properties of UHMWPE/Al<sub>2</sub>O<sub>3</sub> ceramic under different lubricating conditions. *Wear.* 2001;250(1–12):242–5. [https://doi.org/10.1016/S0043-1648\(01\)00647-0](https://doi.org/10.1016/S0043-1648(01)00647-0).
- Gao P, Mackley MR. The structure and rheology of molten ultra-high-molecular-mass polyethylene. *Polymer.* 1994;35(24):5210–6. [https://doi.org/10.1016/0032-3861\(94\)90471-5](https://doi.org/10.1016/0032-3861(94)90471-5).
- Kuram E. Micro-machinability of injection molded polyamide 6 polymer and glass-fiber reinforced polyamide 6 composite. *Compos Part B Eng.* 2016;88:85–100. <https://doi.org/10.1016/j.compositesb.2015.11.004>.
- Campos Rubio JC, Panzera TH, Scarpa F. Machining behaviour of three high-performance engineering plastics. *Proc Inst Mech Eng Part B J Eng Manuf.* 2015;229(1):28–37. <https://doi.org/10.1177/0954405414525142>.
- Wu JJ, Buckley CP, O'Connor JJ. Mechanical integrity of compression-moulded ultra-high molecular weight polyethylene: effects of varying process conditions. *Biomaterials.* 2002;23(17):3773–83. [https://doi.org/10.1016/S0142-9612\(02\)00117-5](https://doi.org/10.1016/S0142-9612(02)00117-5).
- Parasnis NC, Ramani K. Analysis of the effect of pressure on compression moulding of UHMWPE. *J Mater Sci Mater Med.* 1998;9(3):165–72. <https://doi.org/10.1023/A:1008871720389>.
- Gürgen S. Wear performance of UHMWPE based composites including nano-sized fumed silica. *Compos Part B Eng.* 2019;173:106967. <https://doi.org/10.1016/j.compositesb.2019.106967>.
- Gürgen S, Çelik ON, Kuşhan MC. Tribological behavior of UHMWPE matrix composites reinforced with PTFE particles and aramid fibers. *Compos Part B Eng.* 2019;173:106949. <https://doi.org/10.1016/j.compositesb.2019.106949>.
- Carr JW, Feger C. Ultraprecision machining of polymers. *Precis Eng.* 1993;15(4):221–37. [https://doi.org/10.1016/0141-6359\(93\)90105-J](https://doi.org/10.1016/0141-6359(93)90105-J).
- Wang S, Ge S. The mechanical property and tribological behavior of UHMWPE: effect of molding pressure. *Wear.* 2007;263(7–12):949–56. <https://doi.org/10.1016/j.wear.2006.12.070>.
- Sivasakthivel PS, Sudhakaran R. Optimization of machining parameters on temperature rise in end milling of Al 6063 using response surface methodology and genetic algorithm. *Int J Adv Manuf Technol.* 2013;67(9–12):2313–23. <https://doi.org/10.1007/s00170-012-4652-8>.
- Gürgen S, Sofuoğlu MA. Advancements in conventional machining. In: *Advanced machining and finishing*. Amsterdam: Elsevier; 2021. pp. 143–175. <https://doi.org/10.1016/B978-0-12-817452-4.00015-4>.
- Çakır FH, Sofuoğlu MA, Gürgen S. Machining of Hastelloy-X based on finite element modelling. *Adv Eng Forum.* 2018;30:1–7. <https://doi.org/10.4028/www.scientific.net/AEF.30.1>.
- Rashed AH. Properties and characteristics of silicon carbide. Poco Graphite Inc.; 2002. p. 1–19.

**Publisher's Note** Springer Nature remains neutral with regard to jurisdictional claims in published maps and institutional affiliations.